JOURNAL OF MATERIALS SCIENCE 21 (1986) 3648-3652

Properties of Va metal–B films prepared by r.f.-sputtering

Part 2 *Characterization and properties of the films in the system Nb–B*

KIICHI ODA, HIROHIDE YATA*, TETSUO YOSHIO, KAZUO O-OKA
Research Institute for Non-Crystalline Materials, School of Engineering, Okayama University, Okayama 700, Japan

KOHEI ODA
Department of Industrial Chemistry, Yonago Technical College, Yonago 683, Japan

$Nb_{100-x}B_x$ alloy films were prepared by the r.f.-sputtering method in the chemical composition range of $30 \leqq x \leqq 76$. $Nb_{100-x}B_x$ ($30 \leqq x \leqq 54$) films consisted of the amorphous state, and NbB_2 crystal phase was observed on $Nb_{100-x}B_x$ ($67 \leqq x \leqq 76$) films. A remarkable preferred orientation with the (001) plane of NbB_2 in parallel to the film surface was observed on $Nb_{33}B_{67}$ film. d.c. electrical conductivity of $Nb_{100-x}B_x$ ($30 \leqq x \leqq 76$) films decreased with increasing content of boron in the range from 7.3×10^3 to $7.6 \times 10^2 \Omega^{-1} cm^{-1}$. Micro-Vickers hardness of $Nb_{100-x}B_x$ ($30 \leqq x \leqq 76$) films exhibited the values of 1070 to 2060 kg mm^2.

1. Introduction

The borides, especially diborides (ZrB_2, TiB_2, NbB_2, HfB_2 and etc.), are a highly refractory group of non-oxide ceramic materials, which are characterized by extremely high hardness and high electrical conductivity up to high temperature [1]. These borides are favourable as coating materials characterized by not only high hardness and electrical conductivity, but also high chemical durability.

The authors have applied the r.f.-sputtering method to the preparation of borides films in the Ta–B system, and obtained Ta–B films with high hardness and high electrical conductivity [2]. Succeeding to the Ta–B system, the r.f.-sputtering technique has also been applied to the preparation of the coating films in the Nb–B system.

In the present work, Nb–B films were prepared by the r.f.-sputtering method, and the film composition was controlled by the co-sputtering technique. Characterization based on the chemical analysis, X-ray diffractometry, transmission electron microscope (TEM) and scanning electron microscope (SEM) observations were carried out on the Nb–B films. As the characteristic properties of the films, d.c. electrical conductivity and micro-Vickers hardness were also measured, and the compositional dependences of those properties were examined.

2. Experimental details

Nb–B films were prepared by the use of an Ulvac SBR-1104 type r.f.-sputtering apparatus. The co-sputtering technique was employed in order to control the composition of the Nb–B film. A composite target used for co-sputtering was composed of a boron powder disc (99%, 100 mm$^{\phi}$) and geometrically arranged 69 niobium metal chips (99.96%, 4 to 8 mm square) [2]. A composite target was placed on the lower electrode and a substrate was attached on the centre of the upper electrode.

Glass slides and polyimide film were used as substrates. Nb–B film samples for chemical analysis, X-ray diffractometry, SEM observation, d.c. electrical conductivity and micro-Vickers hardness were sputtered onto the glass slides substrates. Nb–B film sample for TEM observation were sputtered onto the polyimide film substrates, and then removed from the polyimide substrate with hydrofluoric acid solution. Sputtering conditions are shown in Table I. Chemical composition of Nb–B films was determined by means of an absorption spectroscopy with pyrogallol for niobium and methylene-blue for boron, respectively. Film thickness was measured by a stylus type surface analyser. d.c. electrical conductivity was measured with the use of four terminals method in the temperature range from -150 to 150° C. Measurement of micro-Vickers hardness was carried out at room temperature with the use of a DMH-2 type micro-Vickers tester (Matsunami Seiki Co., Ltd). Load was 10 g and loading time was 15 sec during the measurement of micro-Vickers hardness, these conditions were chosen by considering the film thickness and the measurement precision.

3. Results and discussion

3.1. Characterization of the film

All Nb–B films had a metallic lustre, and the deposition rate was 4.5 to 6 nm min^{-1} under the present sputtering conditions (Table I). Nb–B films with the

**Present address:* Central Research Laboratory of Ube Industries Ltd, Kogushi 1978-5, Ube 755, Japan.

0022-2461/86 $03.00 + .12 © *1986 Chapman and Hall Ltd.*

TABLE I Sputtering conditions

Target	Nb–B
Substrate	Glass slide, polyimide film
Gas	Argon
Pressure	2×10^{-2} mm Hg
Sputtering power	100 W
Substrate temperature	160° C

thickness of 1 to 3 μm were obtained by sputtering for 4 to 8 h.

The results of chemical analysis for Nb–B films are summarized in Table II.

Plot of area ratio of niobium to boron in target against chemical composition ratio of niobium to boron in the obtained film is shown in Fig. 1. It is found that the ratio of the film increases a little concavely with increasing the target ratio. Nb–B films can be prepared in the compositional range from 30 to 76 at % B. From the results of electron probe X-ray microanalyser (EPMA) analysis for Nb–B films, it was confirmed that the Nb–B film composition was fairly uniform over the film. It is recognized that the co-sputtering technique is available to control the film composition also in this system.

X-ray diffraction patterns of Nb–B film sputtered onto the glass slide substrate for 8 h are shown in Fig. 2. Nb–B–1 (30 at % B) shows a very broad diffraction line around $2\theta = 35°$ for Cu$K\alpha$ radiation, which peak position is corresponding to d_{110} of bcc–Nb metal. Similar X-ray diffraction patterns are observed on Nb–B–2 (43 at % B) and Nb–B–3 (54 at % B). X-ray diffraction lines of Nb–B–4 (67 at % B) are identified to be those of NbB_2 crystal phase, since the film composition is almost equal to the stoichiometric composition of NbB_2. Additionally, a remarkable preferred orientation with (0 0 1) plane of NbB_2 in parallel to the film surface is observed on Nb–B–4 (67 at % B). In the case of the sputtering method, preferred orientation has been sometimes observed on the as-sputtered films, e.g. TaB_2 [2], Co [3], ZnO [4], AlN [5], Ba-hexaferrite [6] and α-Fe_2O_3 [7]. Of these films, crystals with a hexagonal symmetry system tend to grow with the preferred orientation with the (0 0 1) plane in parallel to the film surface during the sputtering on the amorphous (oxide glass) substrate. It can be assumed that the preferred orientation of NbB_2 crystals is caused by the growth rate of the (0 0 1) plane being larger than that of other planes under the present sputtering conditions. Similar preferred orientation has been observed also on the Ta–B film [2]. Beyond 67 at % B, no preferred orientation is observed (Fig. 2e). X-ray diffraction

TABLE II Target constitution as surface area ratio Nb/B and composition of Nb–B sputtered film

Sample No.	Area ratio S_{Nb}/S_B (–)	Film composition (at % B)
Nb–B–1	56/44	30
Nb–B–2	43/57	43
Nb–B–3	32/68	54
Nb–B–4	22/78	67
Nb–B–5	14/86	76

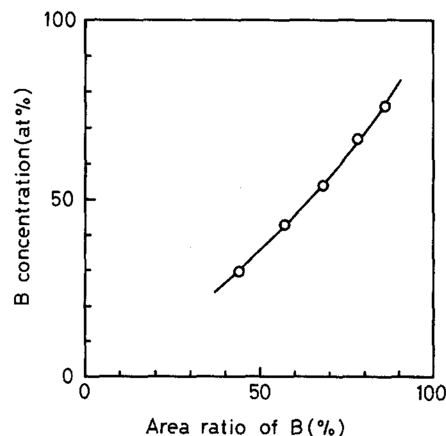

Figure 1 Plot of boron concentration in the film against area ratio of boron to niobium in the target.

pattern of Nb–B–5 (76 at % B) shows the superposition of X-ray amorphous pattern and weak diffraction lines of randomly oriented NbB_2 crystals.

Transmission electron micrographs of Nb–B–1 (30 at % B) as-sputtered film is shown in Fig. 3. Nb–B–1 (30 at % B) film exhibits a representative amorphous pattern. It is found that Nb–B–1 (30 at % B) film consists of the amorphous state.

The results of X-ray diffraction and TEM observation of $Nb_{100-x}B_x$ ($30 \leqq x \leqq 76$) films are entirely similar to that of Ta–B films under the same sputtering conditions [2]. In the case of $Ta_{100-x}B_x$ ($45 \leqq x \leqq 77$) films, the relation between observed phases and the composition of Ta–B films can be well explained by considering phase diagram of Ta–B system and the rapid quenching conditions of sputtering process. The phase diagram in the Nb–B system was determined by Nowotny *et al.* [8]. In Fig. 4, the results of both observed phases and film compositions are

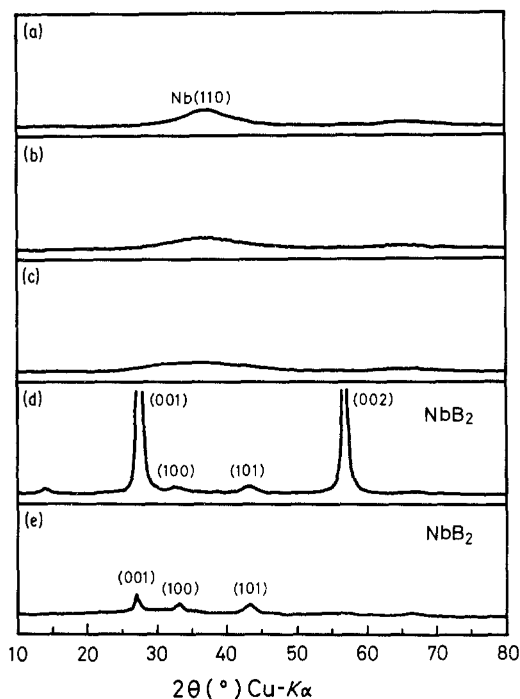

Figure 2 X-ray diffraction patterns of Nb–B film sputtered onto the glass slide substrate. (a) 30 at % B, (b) 43 at % B, (c) 54 at % B, (d) 67 at % B, (e) 76 at % B.

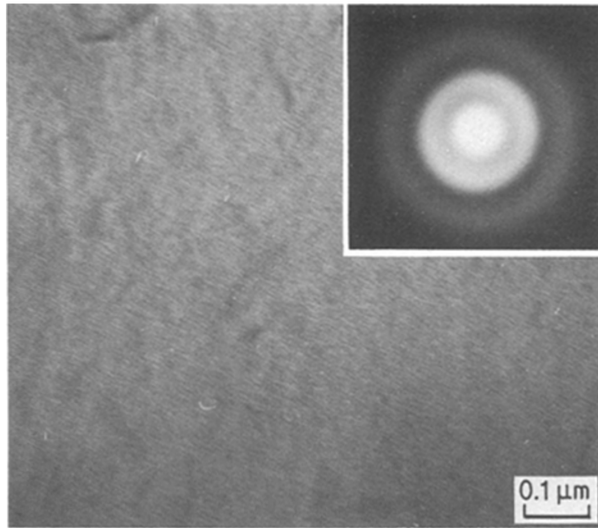

Figure 3 Transmission electron micrograph of Nb–B–1 (30 at % B) film.

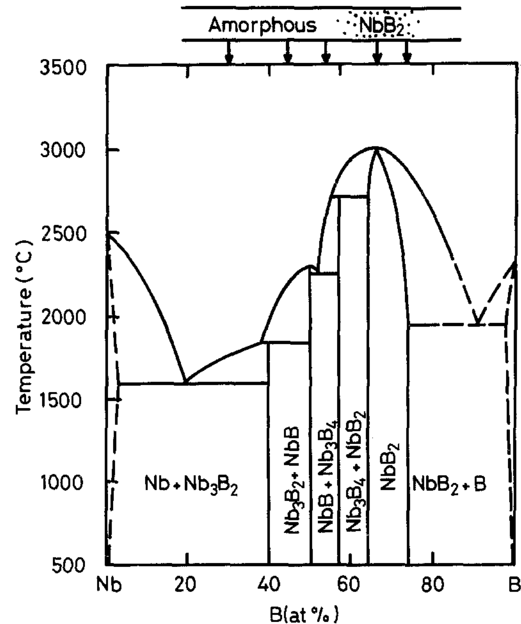

Figure 4 Phase diagram in the system Nb–B and composition of obtained Nb–B film [8].

schematically illustrated in relation to the phase diagram in the Nb–B system. Also in the system Nb–B, low eutectic point ($\cong$ 1600° C) at $\cong$ 20 at % B exists between Nb (m.p. = 2500° C) and NbB_2 (m.p. = 3000° C), and another eutectic point ($\cong$ 1950° C) exists between NbB_2 (m.p. = 3000° C) and boron (m.p. = 2300° C). The liquidus line falls down radically from NbB_2 to the eutectic point on both sides. Consequently, by considering the phase diagram in the Nb–B system and the rapid quenching conditions of the sputtering process, the observed phases of Nb–B films are explained as in the system Ta–B. With respect to the structure, the structure type of transition metal borides are well classified up systematically by space consideration and packing of boron and transition metal atoms [9]. Niobium, tantalum and boron atomic radii in metals and borides are shown in Table III. It is found that the radius of the niobium atom is almost equivalent to that of the tantalum atom even though r (Nb–B) in NbB_2 is a little larger than r (Ta–B) in TaB_2. Accordingly, borides in the Nb–B system give the isomorphous structure of borides in the Ta–B system, except for Me_2B (Me = Ta, Nb) as shown in Table IV. Therefore, observed phases of Nb–B films are just same to those of Ta–B films under the same sputtering conditions.

Scanning electron micrographs of Nb–B–1 (30 at % B) and Nb–B–4 (67 at % B) are shown in Fig. 5. It is found that these films are fairly dense, and no cracks and voids are observed.

3.2. Properties of the films

Temperature dependence of d.c. conductivity of $Nb_{100-x}B_x$ ($30 \leqq x \leqq 76$) films in the temperature range from – 150 to 150° C is shown in Fig. 6. All film samples exhibit metallic conductivity, and the conductivities are independent of temperature in the range from – 150 to 150° C. d.c. conductivity of Nb–B films gradually decreases with increasing boron content in the range from 7.3×10^3 to $7.6 \times 10^2 \Omega^{-1} cm^{-1}$. Clougherty and Pober [16] reported that NbB_2 single crystal (zone refined bar) showed a value of $14.7 \times 10^3 \Omega^{-1} cm^{-1}$ at 25° C. However, present Nb–B–4 (67 at % B) film with the preferred orientation of the (0 0 1) plane in parallel to the film surface exhibits about half the value of NbB_2 single crystals. d.c. electrical conductivity of $Nb_{100-x}B_x$ ($30 \leqq x \leqq 76$) films is of the order of that of $Ta_{100-x}B_x$ ($45 \leqq x \leqq 77$) films, and the compositional dependence of d.c. electrical conductivity of Nb–B films changes almost in the same manner as that of Ta–B films.

Fig. 7 shows the relation between micro-Vickers hardness and Nb–B film composition at room temperature. The films were sputtered onto the glass slide substrates, and the thickness of the films was 2 to 3 μm. The glass slide exhibited the hardness of 530 kg mm^{-2}. The hardness of $Nb_{100-x}B_x$ ($30 \leqq x \leqq 54$) increases with increasing boron content in the range from 1960 to 2060 kg mm^{-2}. While, the hardness of $Nb_{100-x}B_x$ ($54 \leqq x \leqq 76$) decreases with increasing boron content in the range form 2060 to 1070 kg mm^{-2}, then the value of micro-Vickers hardness of Nb–B films attains to a maximum value (2060 kg mm^{-2}) at the composition of $Nb_{46}B_{54}$. This may be caused by the amorphous state of the film, because of there being no grain boundaries, and because the film composition is close to that of NbB_2.

TABLE III Interatomic distances in metal and metal diborides [10]

Metal	r(Me) in metal C.N. in brackets (nm)	r(Me) for C.N. = 12 (nm)	r(Me) (C.N. = 12) + r(B)* (nm)	r(Me–B) obs. in MeB_2 (nm)
Nb	0.143 (8)	0.148	0.235	0.243
Ta	0.143 (8)	0.148	0.235	0.241

* r(B) = 0.087 nm.

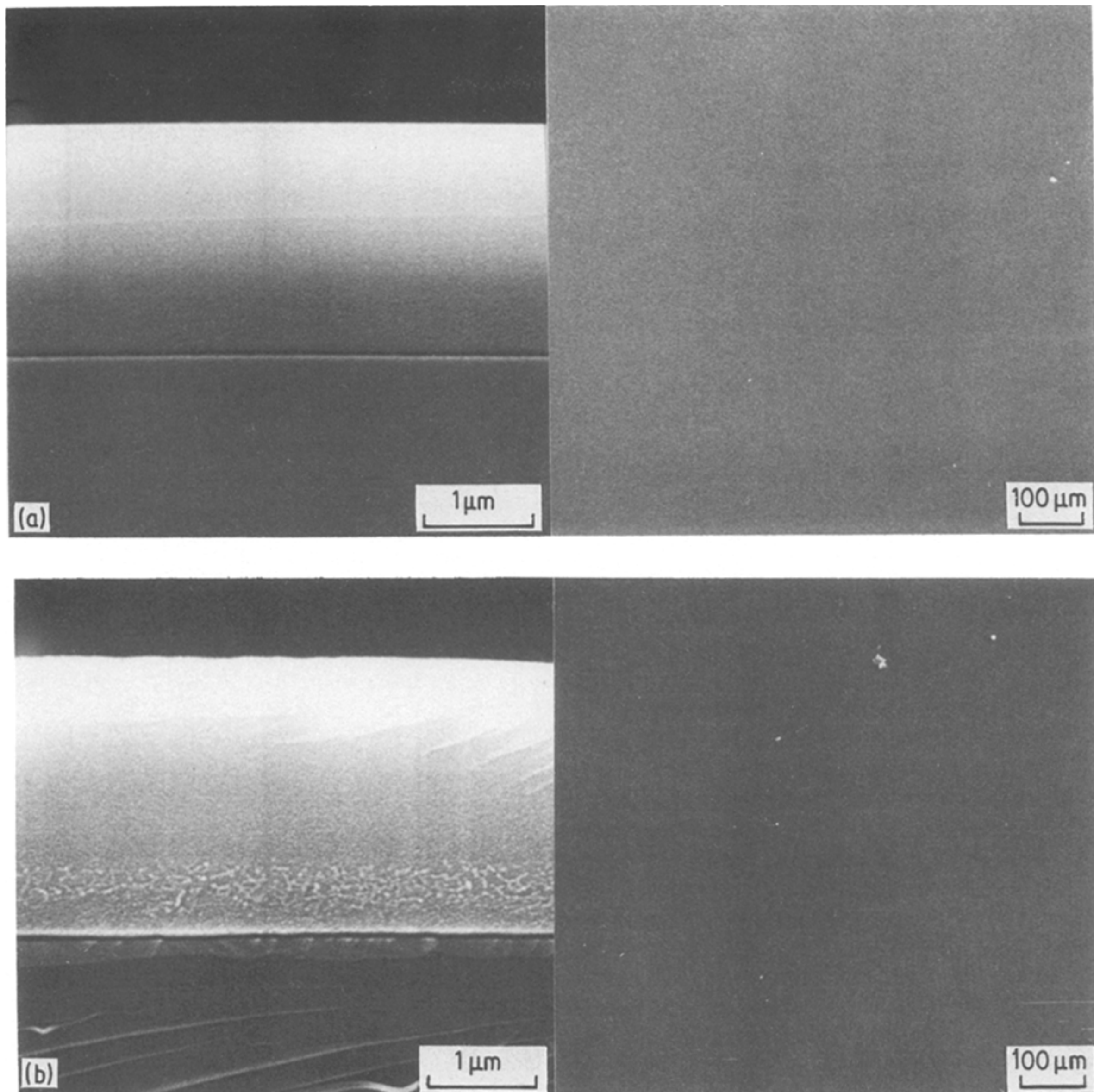

Figure 5 Scanning electron micrographs of fracture surface and film surface of Nb–B film. (a) Nb–B–1 (30 at % B), (b) Nb–B–4 (67 at % B).

The compositional dependence of micro-Vickers hardness of Nb–B films changes in the similar manner as that of Ta–B sputtered films [2], however those values of Nb–B films are a little lower than that of Ta–B films over the whole compositional range.

4. Conclusion

1. The r.f.-sputtering method was applied to the preparation of coating film in the system Nb–B using co-sputtering technique. $Nb_{100-x}B_x$ alloy films with the composition range of $30 \leqq x \leqq 76$ were obtained. Nb–B films consisted of amorphous phase in the composition range of $30 \leqq x \leqq 76$.

2. A remarkable preferred orientation was observed in $Nb_{33}B_{67}$ film, which consisted of NbB_2 with the (0 0 1) plane in parallel to the film surface.

TABLE IV Comparison of crystal phases between in the system Nb–B and in the system Ta–B

Crystal phase Nb–B	Ta–B
Nb (cubic; a = 0.33066 nm) [11]	Ta (cubic; a = 0.33058 nm) [13]
–	Ta_2B (tetragonal; a = 0.5778 nm, c = 0.4864 nm) [14]
Nb_3B_2 (tetragonal; a = 0.6185 nm, c = 0.3280 nm) [11]	Ta_3B_2 (tetragonal; a = 0.6184 nm, c = 0.3286 nm) [15]
NbB (orthorhombic; a = 0.3292 nm, b = 0.8713 nm, c = 0.3165 nm) [12]	TaB (orthorhombic; a = 0.3276 nm, b = 0.8669 nm, c = 0.3157 nm) [14]
Nb_3B_4 (orthorhombic; a = 0.33 nm, b = 1.41 nm, c = 0.313 nm) [12]	Ta_3B_4 (orthorhombic; a = 0.329 nm, b = 1.40 nm, c = 0.313 nm) [14]
NbB_2 (hexagonal; a = 0.3110 nm, c = 0.3264 nm) [12]	TaB_2 (hexagonal; a = 0.3078 nm, c = 0.3265 nm) [14]

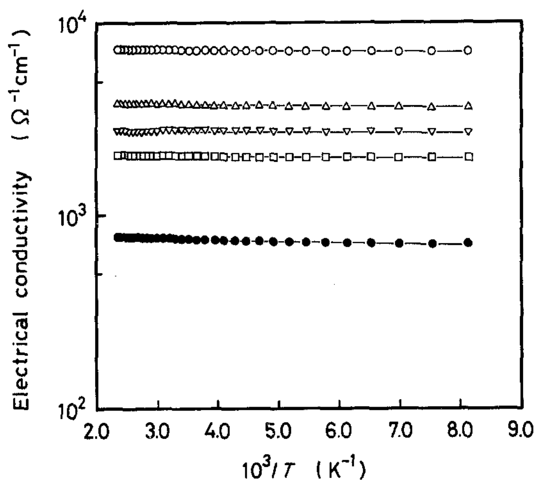

Figure 6 Temperature dependence of d.c. electrical conductivity of Nb–B film. (○) 30 at % B, (△) 43 at % B, (▽) 54 at % B, (□) 67 at % B, (●) 76 at % B.

3. Observed phases almost coincided with that of Ta–B sputtered films.

4. d.c. electrical conductivity of Nb–B films was metallic and almost independent of temperature in the range from -150 to $150°$ C, and decreased with increasing boron content in the range from 7.3×10^3 to $7.6 \times 10^2 \Omega^{-1} cm^{-1}$. d.c. electrical conductivity of Nb–B films was of the order of that of Ta–B films.

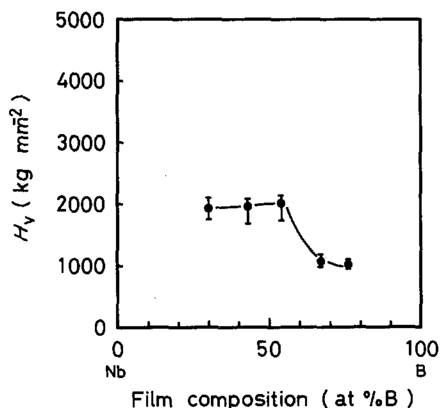

Figure 7 Micro-Vickers hardness of Nb–B film sputtered onto the glass slide substrate for 8 h, film thickness: 2 to 3 μm, load: 10 g (glass slide substrate; $H_v = 530 \text{kg mm}^{-2}$).

5. Micro-Vickers hardness of $Nb_{100-x}B_x$ exhibited the value of 1070 to 2060kg mm^{-2}, these values were relatively lower than that of Ta–B films. $Nb_{46}B_{54}$ film showed a maximum value of 2060kg mm^{-2}, this might be caused by the amorphous state, because no grain boundary existed and that the composition was close to NbB_2.

References

1. P. SCHWALTKOPF and R. KIEFFER (in collaboration with W. LESZYNSKI and F. BENESOVSKY), in "Refractory Hard Metal-Borides, Carbides, Nitrides, and Silicides" (Macmillan, New York, 1953) p. 271.
2. K. ODA, H. YATA, T. YOSHIO, K. O-OKA and K. ODA, *J. Mater. Sci.* **21** (1986) 637.
3. S. IWASAKI and Y. OUCHI, *IEEE Trans. Mag.* **MAG-14** (1978) 849.
4. K. OHJI, T. TOHDA, K. WASA and S. HAYAKAWA, *J. Appl. Phys.* **47** (1976) 1726.
5. A. J. SHUSKUS, T. M. REEDER and E. L. PARADIS, *Appl. Phys. Lett.* **24** (1974) 155.
6. M. NAOE, S. HASUNUMA, Y. HOSHI and S. YAMANAKA, *IEEE Trans. Mag.* **MAG-17** (1981) 3184.
7. R. MESSIER and R. ROY, *J. Non-Cryst. Solids* **28** (1978) 107.
8. H. NOWOTNY, F. BENESOVSKY and R. KIEFFER, *Z. Metallkde.* **50** (1959) 417.
9. A. F. WELLS, in "Structural Inorganic Chemistry" (Clarendon Press, Oxford, 1975) p. 833.
10. B. POST, F. W. GLASER and D. MOSKOWITZ, *Acta Metall.* **2** (1954) 20.
11. JCPDS: International Centre for Diffraction Data, Powder Diffraction File; 16–1, 12–111.
12. L. BREWER, D. L. SAWYER, D. H. TEMPLETON and C. H. DAUBEN, *J. Amer. Ceram. Soc.* **34** (1951) 173.
13. JCPDS: International Centre for Diffraction Data, Powder Diffraction File; 12–99.
14. R. KIESSLING, *Acta Chem. Scand.* **3** (1949) 603.
15. JCPDS: International Centre for Diffraction Data, Powder Diffraction File; 4–788.
16. E. V. CLOUGHERTY and R. L. POBER, *Nucl. Metall.* **10** (1964) 423.

Received 21 October and accepted 20 December 1985